Contents lists available at ScienceDirect

Journal of Ginseng Research

journal homepage: http://www.ginsengres.org

Research article

Ginsenoside Rb1 and compound K improve insulin signaling and inhibit ER stress-associated NLRP3 inflammasome activation in adipose tissue

Weijie Chen, Junlian Wang, Yong Luo, Tao Wang, Xiaochun Li, Aiyun Li, Jia Li, Kang Liu, Baolin Liu*

Jiangsu Key Laboratory of TCM Evaluation and Translational Research, Department of Pharmacology of Chinese Materia Medica, China Pharmaceutical University, Nanjing, China

ARTICLE INFO

ABSTRACT

Background: This study was designed to investigate whether ginsenoside Rb1 (Rb1) and compound K (CK) ameliorated insulin resistance by suppressing endoplasmic reticulum (ER) stress-induced inflammation in adipose tissue.
Methods: To induce ER stress, epididymal adipose tissue from mice or differentiated 3T3 adipocytes were exposed to high glucose. The effects of Rb1 and CK on reactive oxygen species production, ER stress, TXNIP/NLRP3 inflammasome activation, inflammation, insulin signaling activation, and glucose uptake were detected by western blot, emzyme-linked immunosorbent assay, or fluorometry.
Results: Rb1 and CK suppressed ER stress by dephosphorylation of IRE1α and PERK, thereby reducing TXNIP-associated NLRP3 inflammasome activation in adipose tissue. As a result, Rb1 and CK inhibited IL-1β maturation and downstream inflammatory factor IL-6 secretion. Inflammatory molecules induced insulin resistance by upregulating phosphorylation of insulin receptor substrate-1 at serine residues and impairing insulin PI3K/Akt signaling, leading to decreased glucose uptake by adipocytes. Rb1 and CK reversed these changes by inhibiting ER stress-induced inflammation and ameliorating insulin resistance, thereby improving the insulin IRS-1/PI3K/Akt-signaling pathway in adipose tissue.
Conclusion: Rb1 and CK inhibited inflammation and improved insulin signaling in adipose tissue by suppressing ER stress-associated NLRP3 inflammation activation. These findings offered novel insight into the mechanism by which Rb1 and CK ameliorate insulin resistance in adipose tissue.

1. Introduction

The management of diabetes faces the challenge of insulin resistance, which is characterized by impaired insulin signaling. In adipose tissue, insulin promotes glucose uptake by adipocytes through the insulin receptor substrate-1 (IRS-1)/PI3K/Akt pathway. The negative impact of hyperglycemia on insulin-mediated glucose disposal has been well documented [1,2], and evidence shows that oxidative stress is implicated in hyperglycemia-induced insulin resistance [3]. Although it is well known that glucotoxicity-associated oxidative stress, inflammation, and mitochondrial

dysfunction contribute to insulin resistance [4], accumulating evidence shows that endoplasmic reticulum (ER) stress may act as a common mechanism for these events [5]. More than a site for protein folding, the ER functions as a signal-transducing organelle that mediates response to changes in cellular homeostasis by initiating downstream signaling cascades. Sustained cellular stress or metabolic disorders evoke ER stress through increased unfolded-protein response and initiate a stress cascade with pathological consequences that include inflammation in specialized tissues, such as adipose tissue [6,7]. The NLRP3 inflammasome is a molecular platform for immune response that promotes IL-1β

maturation and secretion following cleavage by activated caspase-1 [8]. Recently, the NLRP3 inflammasome was demonstrated to be activated by ER stress and responsible for inflammation and oxidative stress [9]. Pro-inflammatory cytokines, including IL-1β, cause insulin resistance by impairing insulin IRS-1/PI3K/Akt/GLUT4 signaling [10]. High levels of extracellular glucose trigger IL-1β secretion via the NLRP3 inflammasome [11], and blocking IL-1β prevents inflammation and insulin resistance in adipose tissue [12,13], indicating the special role of NLRP3 inflammasome activation in the development of insulin resistance.

Ginsenosides are the major active constituents responsible for the pharmacological properties of ginseng. The ginsenoside Rb1 (Rb1) from *Panax ginseng* root is the most abundant ginsenoside, and ginsenoside compound K (CK) is generated from Rb1 via ginsenoside F2 (Fig. 1) by intestinal bacteria after oral administration [14]. Rb1 shows anti-obesity and antihyperlycemic effects by reducing food intake and body weight in rats [15] and enhancing insulin-mediated glucose uptake in 3T3-L1 adipocytes [16], demonstrating its antidiabetic effect. Similarly, ginsenoside CK also exerts beneficial effects on glucose and lipid metabolism, as well as insulin sensitivity in diabetic rats [17]. Despite these studies showing the actions of Rb1 and CK in the improvement of insulin sensitivity, the potential molecular targets or pathways remain unknown. Rb1 and CK inhibit inflammatory and oxidative responses [18–20], however, whether this action contributes to ameliorating insulin resistance remains to be determined. In the present study, we induced ER stress-associated inflammation by exposing adipose tissue or adipocytes to high glucose insult, and observed the effects of ginsenoside Rb1 and its metabolite CK on insulin PI3K signaling, with emphasis on the inhibition of NLRP3 inflammasome activation in the setting of ER stress. Our results indicated that Rb1, as well as CK, suppressed ER stress and subsequent TXNIP/NLRP3 inflammasome activation, and therefore ameliorated insulin resistance by facilitating insulin PI3K signaling. These findings elucidated the link between ER stress and insulin resistance in adipose tissue, and presented a novel mechanism through which Rb1 and CK inhibit inflammation and ameliorate insulin resistance under ER stress conditions.

2. Materials and methods

2.1. Materials

Rb1 (98% purity) and CK (98% purity) were obtained from State Key Laboratory of Natural Medicines (China Pharmaceutical University, Nanjing, Jiangsu, China). The following items were purchased from the cited commercial sources: insulin, tauroursodeoxycholic acid (TUDCA), thapsigargin (TG), diphenyleneiodonium chloride (DPI), Dulbecco's *ad libitum* Minimum Essential Medium (DMEM), fetal bovine serum (FBS), and β-mercaptoethanol from Sigma-Aldrich (St Louis, MO, USA); Anti-IL-1β antibody (MAB201) from R&D (Minneapolis, MN, USA); Bovine serum albumin (BSA) from Nanjing Sunshine Biotechnology Co., Ltd. (Nanjing, Jiangsu, China); Bicinchoninic Acid Protein Assay kit from Biosky Biotechnology Corporation (Nanjing, Jiangsu, China); Enhanced Chemiluminescence (ECL) Western Blotting Detection System from Beyotime Institute of Biotechnology (Haimen, Jiangsu, China); Reactive Oxygen Species Assay kit (DCFH-DA) from Beyotime Institute of Biotechnology (Shanghai, China). Monoclonal antibodies were procured from the cited commercial sources: anti-TXNIP (NBP1-54578) and anti-NLRP3 (NBP2-12446), Novus Biologicals (Littleton, CO, USA); anti-PERK (#3192), Cell Signaling Technology (Beverly, MA, USA); anti-phospho-PERK (Thr 981; sc-32577) and anti-phospho-IRS-1 (PY99; sc-7020), Santa Cruz Biotechnology, Inc. (Dallas, TX, USA); anti-phospho-IRE1α (S724; ab104157) and anti-IRE1α (ab37073), Abcam (Cambridge, MA, USA); anti-phospho-IRS-1 (Ser307; BS4104), anti-IRS-1 (BS1408), anti-phospho-Akt (T308; BS40080), anti-Akt (BS1810), anti-GAPDH (AP0063), and goat anti-mouse IgG (H+L) horseradish peroxidase (HRP; BS12478), Bioworld Technology (St. Paul, MN,USA).

2.2. Animals

Male Institute for Cancer Research mice (18−22 g) were supplied by the Laboratory Animal Center of Nanjing Qinglongshan. The animal care and experimental procedures were approved by Animal Ethics Committee of School of Chinese Materia Medica,
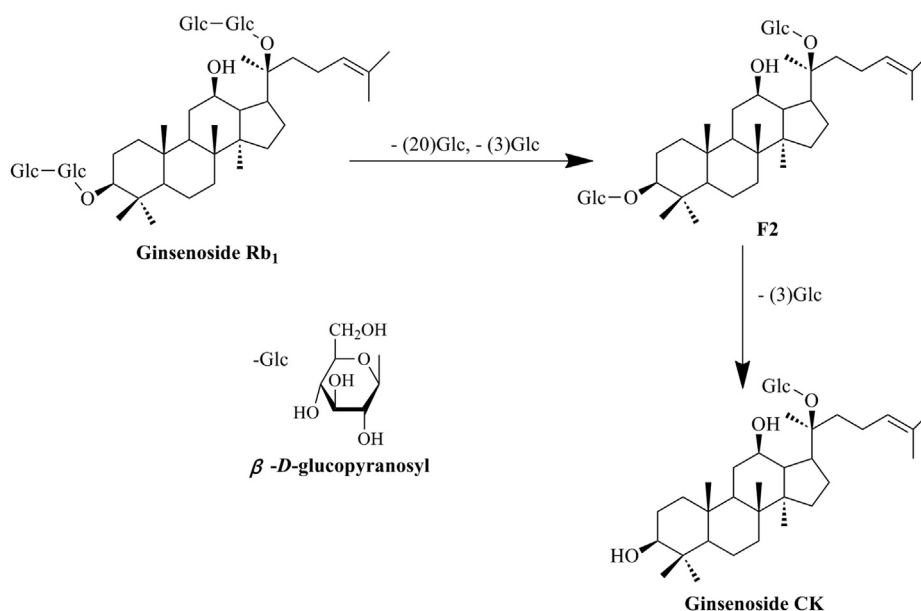
Fig. 1. Structures of ginsenoside Rb1 and compound K. Ginsenoside CK is generated from ginsenoside Rb1 by eliminating the C-20 and two C-3 sugar chains following hydrolysis by intestinal bacteria after oral administration. CK, ginsenoside compound K.

China Pharmaceutical University. Animals were housed in a room with a constant temperature ($22 \pm 1°C$) and were maintained on a standard diet and water *ad libitum*.

2.3. Cell culture and differentiation

3T3-L1 adipocyte cells (the cell bank of the Chinese Academy of Sciences, Shanghai, China), a cell line of preadipocytes, were cultured in 5mM glucose DMEM with 10% (v/v) FBS supplemented with streptomycin (100 μg/mL) and penicillin (100 U/mL) at 37°C under an humidified atmosphere of 5% CO_2. Post-confluent cells were differentiated by incubation in DMEM with 10% FBS containing insulin (0.1μM), isobutylmethylxanthine (0.5mM), and dexamethasone (1mM) for 2 days, then incubated for an additional 2 days in DMEM with 10% FBS containing 0.1μM insulin alone until over 80% of the cells exhibiting the mature adipocyte phenotype with large lipid droplets were apparent in the cytoplasm.

### 2.4. Western blot analysis of protein in adipose tissue

Mice were sacrificed by cervical dislocation, and epididymal adipose tissue was separated. Equal amounts of adipose tissue were dissected and rinsed in phosphate-buffered saline (PBS), incubated in 5mM DMEM supplemented with 10% FBS, and pretreated with Rb1 (10μM), CK (10μM), Rb1 (5μM)+CK (5μM), TUDCA (200μM), or anti-IL-1β antibody (0.06 μg/mL) individually in the presence or absence of high glucose (33mM) for 24 h, or TG (1μM) for 12 h. Furthermore, the tissue used for detecting the insulin signaling pathway was treated with insulin (0.1μM) for an additional 30 min. After incubation, adipose tissue was homogenized in ice-cold lysis buffer in order to extract the protein. Homogenates were centrifuged at 12,000g for 15 min at 4°C, and supernatants were collected. The protein concentration of each sample was determined using a Bicinchoninic Acid Protein Assay kit. Equal amounts of protein were separated by SDS-PAGE and transferred to polyvinylidene fluoride (PVDF) membranes. After incubation with primary antibodies overnight at 4°C, the PVDF membranes were incubated with secondary antibodies for 2 h at room temperature. Antibody-antigen complexes were detected by ECL and quantized by densitometry with Image-Pro Plus 6.0 software (MediaCybernetics, Rockville, MD, USA).

2.5. Measurement of reactive oxygen species (ROS) production in adipose tissue

Epididymal adipose tissue was separated after the mice were sacrificed. The tissue was cultured in 48-well plates ($\sim$70 mg/well) with the indicated agents and in the presence or absence of high glucose (33mM) for 24 h, or TG (1μM) for 12 h. The tissue was homogenized with PBS to extract the protein, and the homogenate was centrifuged at 3000g for 5 min at 4°C. The supernatant was collected for the determination of ROS using enzyme-linked immunosorbent assay (ELISA) kits (Dizhao Biotec, Shanghai, China). After treatment, the tissue was incubated with ROS-specific fluorescent-probe dye dichloro-dihydro-fluorescein diacetate (DCFH-DA; Beyotime Institute of Biotechnology) for 0.5 h at 37°C, and ROS production was measured using a microplate reader at an excitation/emission wavelength of 488/525 nmnm.

2.6. Assay of IL-1β, IL-6 activity in adipose tissue

Mice were sacrificed by cervical dislocation, and epididymal adipose tissue was separated. The tissue was cultured in six-well plates ($\sim$150 mg/well) and pretreated with Rb1 (10μM), CK (10μM), Rb1 (5μM)+CK (5μM), TUDCA (200μM), or DPI (1μM) in the
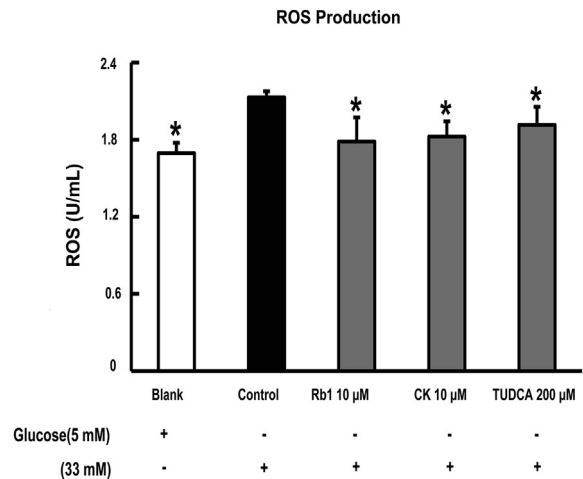
Fig. 2. Rb1 and CK inhibit ROS production in adipose tissue. Epididymal adipose tissue was separated from mice, cultured with Rb1 (10μM), CK (10μM), TUDCA (200μM), and then stimulated with high glucose (33mM) for 24 h. ROS production in the tissue was determined with an ELISA kit. Data were expression as mean $\pm$ SD from three independent experiments. *$p < 0.05$ versus high glucose-only treatment. CK, ginsenoside compound K; ROS, reactive oxygen species, SD, standard deviation.

presence or absence of high glucose (33mM) for 24 h, or TG (1μM) for 12 h. The supernatant was collected and centrifuged at 3000g for 5 min at 4°C, and the levels of IL-1β and IL-6 in the supernatant were assayed using commercial ELISA kits (Dizhao Biotec, Shanghai, China) following manufacturer protocol.

2.7. PI3K activity assay in adipose tissue

Mice were sacrificed by cervical dislocation, and epididymal adipose tissue was separated. The tissue was cultured in six-well plates ($\sim$150 mg/well) and treated with Rb1, CK, or TUDCA at the given concentrations in the presence or absence of high glucose (33mM) for 24 h, followed by treatment with insulin (0.1μM) for an additional 30 min. To extract protein, the tissue was homogenized in lysis buffer, the homogenate was centrifuged at 12,000g for 20 min at 4°C, and the supernatant was collected for the determination of PI3K with an ELISA kit (Dizhao Biotec, Shanghai, China) according to manufacturer instructions.

2.8. Glucose uptake assay in 3T3-L1 adipocytes

The 3T3-L1 adipocytes were cultured in 48-well plates to 80% confluency and starved for 4 h in Krebs Ringer HEPES (KRH) buffer. Cells were exposed to Rb1 (10μM), CK (10μM), or TUDCA (200μM) for 30 min, then stimulated with high glucose (33mM) for 24 h. After treatment, cells were incubated with a fluorescent probe (2-D-deoxyglucose-specific fluorescent dye, 2-NDBG) in the presence or absence of insulin (0.1μM) in the dark at 37°C for 30 min. Cells were then washed three times with KRH to remove the unconjugated dye, and fixed in 4% paraformaldehyde at 4°C for 5 min. Fluorescence in the cells was examined using a fluorescence microscope, and the degree of fluorescence was quantized by densitometry with Image-Pro Plus 6.0 software (MediaCybernetics).

2.9. Statistical analysis

Results are expressed as mean $\pm$ standard deviation (SD). Data were analyzed using the Student t test or one-way analysis of variance, followed by a Newman-Keuls test. Values of $p < 0.05$ were considered statistically significant (Concise Statistics, version 14.0).

3. Results

3.1. Rb1 and CK inhibit ROS production in adipose tissue

We first observed the effect of Rb1 and CK on ROS generation in adipose tissue. Fig. 2A shows that ROS production increased markedly when adipose tissue was exposed to high glucose challenge. Rb1 and CK decreased ROS production, demonstrating their antioxidant activity in adipose tissue. Furthermore, the ER-stress inhibitor TUDCA suppressed ROS production, indicating the involvement of ER stress in high glucose insult.

3.2. Rb1 and CK inhibit ER stress in adipose tissue

To examine whether high glucose concentrations induced ER stress in adipose tissue, we examined the activation of IRE1α and PERK, which are indicators of ER stress, in epididymal adipose tissue exposed to high glucose concentrations. As shown in Fig. 3A, high glucose stimulation increased IRE1α phosphorylation, but this alteration was reversed by treatment with Rb1 and CK. Similarly, Rb1 and CK treatment attenuated glucose-induced PERK phosphorylation (Fig. 3B). These results indicated that Rb1, as well as CK, suppressed ER stress in adipose tissue. TUDCA also effectively attenuated IRE1α and PERK phosphorylations.

3.3. Rb1 and CK inhibit TXNIP induction in adipose tissue

To determine whether ROS-associated ER stress could induce TXNIP activation, we next observed TXNIP expression in adipose tissue, and found that TXNIP expression increased following glucose insult. However, pretreatment with Rb1 and CK attenuated TXNIP expression, demonstrating their ability to suppress TXNIP activation. Similar to Rb1 and CK, ER-stress inhibitor TUDCA also reduced TXNIP expression in adipose tissue (Fig. 4).

3.4. Rb1 and CK prevent NLRP3 inflammasome activation

TXNIP induction is essential for NLRP3 inflammasome complex activation. Therefore, we investigated NLRP3 inflammasome activation in response to glucose load. Rb1 and CK inhibited NLRP3 expression following glucose challenge (Fig. 5A). Moreover, we also observed that Rb1 and CK prevented the cleavage of pro-caspase-1, indicated by attenuated levels of cleaved caspase-1 (Fig. 5B). These
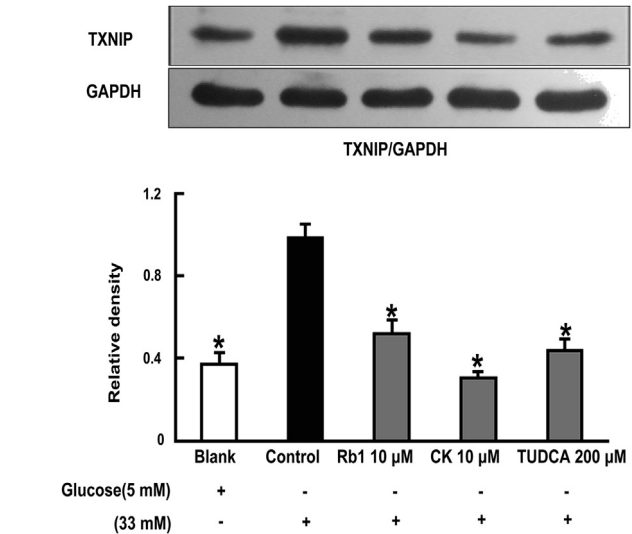

Fig. 4. Rb1 and CK attenuate TXNIP expression in adipose tissue. Epididymal adipose tissue was separated after the mice were sacrificed. The tissue was pretreated with Rb1, CK, or TUDCA at given the concentrations, and exposed to high glucose (33mM) for 24 h. The expression of TXNIP was determined by western blot. Data were expressed as mean ± SD from three independent experiments. *$p < 0.05$ versus high glucose-only treatment. CK, ginsenoside compound K; SD, standard deviation; TUDCA, tauroursodeoxycholic acid.

results demonstrated that NLRP3 inflammasome activation was inhibited by Rb1 and CK treatment. TUDCA also effectively prevented NLRP3 inflammasome activation by attenuating NLRP3 expression and cleaved caspase-1 levels, indicative of the role of ER stress in NLRP3 inflammasome activation.
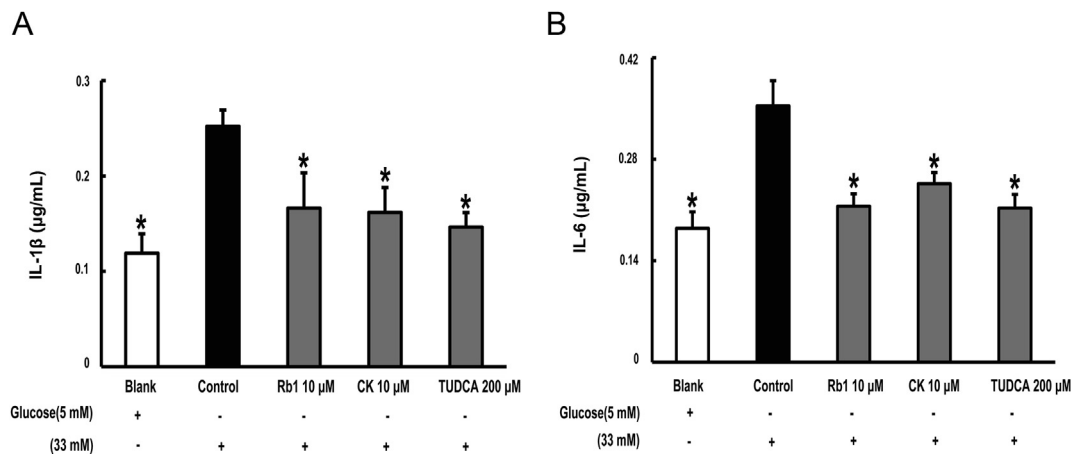
3.5. Rb1 and CK inhibit inflammation in adipose tissue

IL-1β maturation is mediated by the NLRP3 inflammasome through cleavage of caspase-1. High glucose exposure increased the secretion of IL-1β, and this change was prevented by Rb1 and CK treatment (Fig. 6A). As a major downstream product of IL-1β, IL-6 secretion increased in response to glucose insult. Rb1 and CK, as well as TUDCA, reduced IL-6 production, suggesting their anti-inflammatory effects (Fig. 6B).
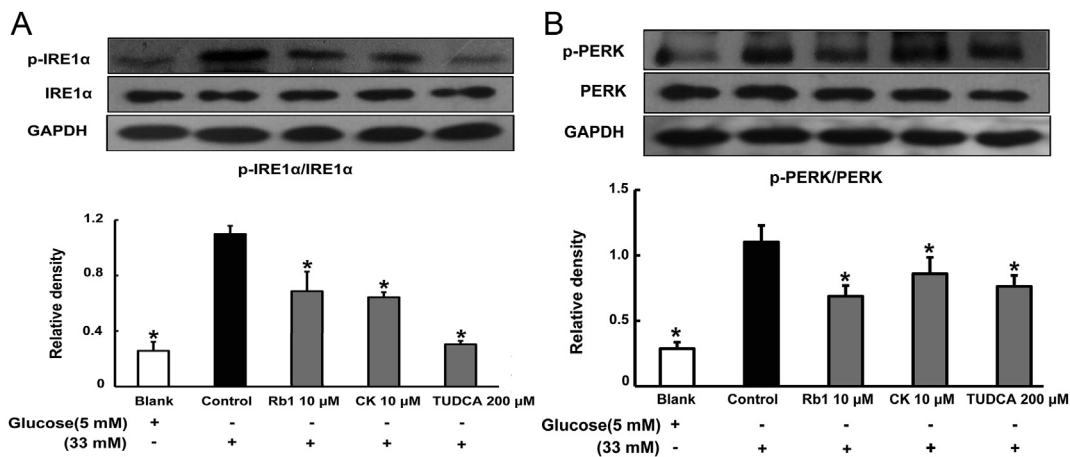
Fig. 3. Rb1 and CK inhibit ER stress in adipose tissue. Mice were sacrificed by cervical dislocation, and epididymal adipose tissue was separated. The tissue was pretreated with Rb1 (10μM), CK (10μM), or TUDCA (200μM), and then cultured with high glucose (33mM) for 24 h. IRE1α (A) and PERK (B) phosphorylation was determined by western blot. The results were expressed as the mean ± SD of three independent experiments. *$p < 0.05$ versus high glucose-only treatment. CK, ginsenoside compound K; ER, endoplasmic reticulum; SD, standard deviation; TUDCA, tauroursodeoxycholic acid.
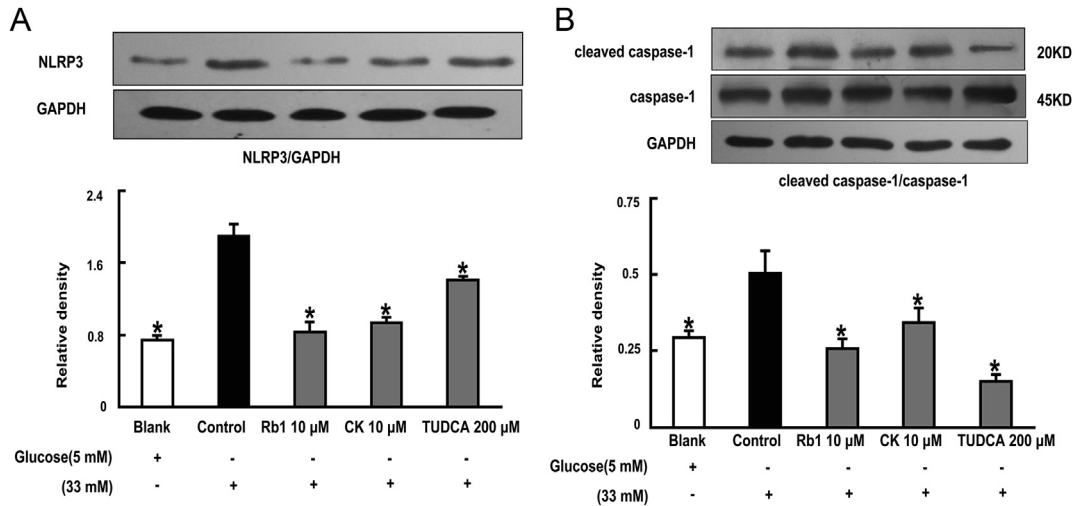
Fig. 5. NLRP3 inflammasome activation in adipose tissue was prevented by Rb1 and CK. Epididymal adipose tissue was pretreated with Rb1 (10μM), CK (10μM), or TUDCA (200μM), and then stimulated with high glucose (33mM) for 24 h. NLRP3 (A) expression and cleaved caspase-1 (B) protein levels were determined by western blot. The results were expressed as the mean ± SD of three independent experiments. *$p < 0.05$ versus high glucose-only treatment. CK, ginsenoside compound K; SD, standard deviation; TUDCA, tauroursodeoxycholic acid.

Fig. 6. Rb1 and CK inhibit inflammation in adipose tissue. Epididymal adipose tissue was separated and stimulated with glucose in the presence of Rb1, CK, or TUDCA. IL-1β (A) and IL-6 (B) in the supernatant were measured with ELISA kits. The results were expressed as the mean ± SD ($n = 4$). *$p < 0.05$ versus high glucose-only treatment. CK, ginsenoside compound K; ELISA, enzyme-linked immunosorbent assay; SD, standard deviation; TUDCA, tauroursodeoxycholic acid.

3.6. Rb1 and CK modulate IRS-1 phosphorylation in the presence of high glucose concentrations

To determine the impact of inflammation on insulin signaling, we observed the phosphorylation of IRS-1 in adipose tissue subjected to glucose exposure. High glucose concentrations enhanced phosphorylation of IRS-1 at a serine residue (S307) and reduced insulin-mediated tyrosine phosphorylation (detected by PY99), whereas these alternations were reversed by treatment with Rb1 and CK (Figs. 7A and 7B). As a result of beneficial regulation of IRS-1 phosphorylation, Rb1 and CK treatment effectively increased insulin-induced PI3K activity (Fig. 7C). TUDCA exhibited similar regulatory behavior toward the insulin IRS-1/PI3K signaling pathway as that observed from Rb1 and CK.

3.7. Rb1 and CK enhance Akt phosphorylation and promote insulin-mediated glucose uptake

Akt activation is essential for insulin-mediated glucose uptake. High glucose concentrations impaired insulin PI3K signaling and inhibited Akt activation, indicated by Akt dephosphorylation. Pre-treatment of adipose tissue with Rb1 and CK effectively restored insulin-mediated Akt phosphorylation in adipose tissue exposed to high glucose concentrations (Fig. 8A). As expected, we also observed that Rb1 and CK promoted insulin-mediated glucose uptake by adipocytes (Fig. 8B). TUDCA also increased Akt phosphorylation and promoted glucose uptake by adipocytes.

3.8. Rb1 and CK in combination improve insulin signaling

Given that CK is a metabolic product of Rb1 and both simultaneously present in the blood, we investigated the effects of combined Rb1 and CK on the regulation of insulin signaling in the setting of ER stress. ER-stress inducer thapsigargin (TG) promoted ROS generation, increased IL-1β production, and impaired insulin signaling, indicated by the inhibition of insulin-mediated Akt phosphorylation. Neutralizing IL-1β with anti-IL-1β antibody effectively preserved insulin-mediated Akt activation, indicating ER stress-associated NLRP3 inflammasome activation was responsible for the impairment of insulin signaling. Similar to Rb1 and CK, the
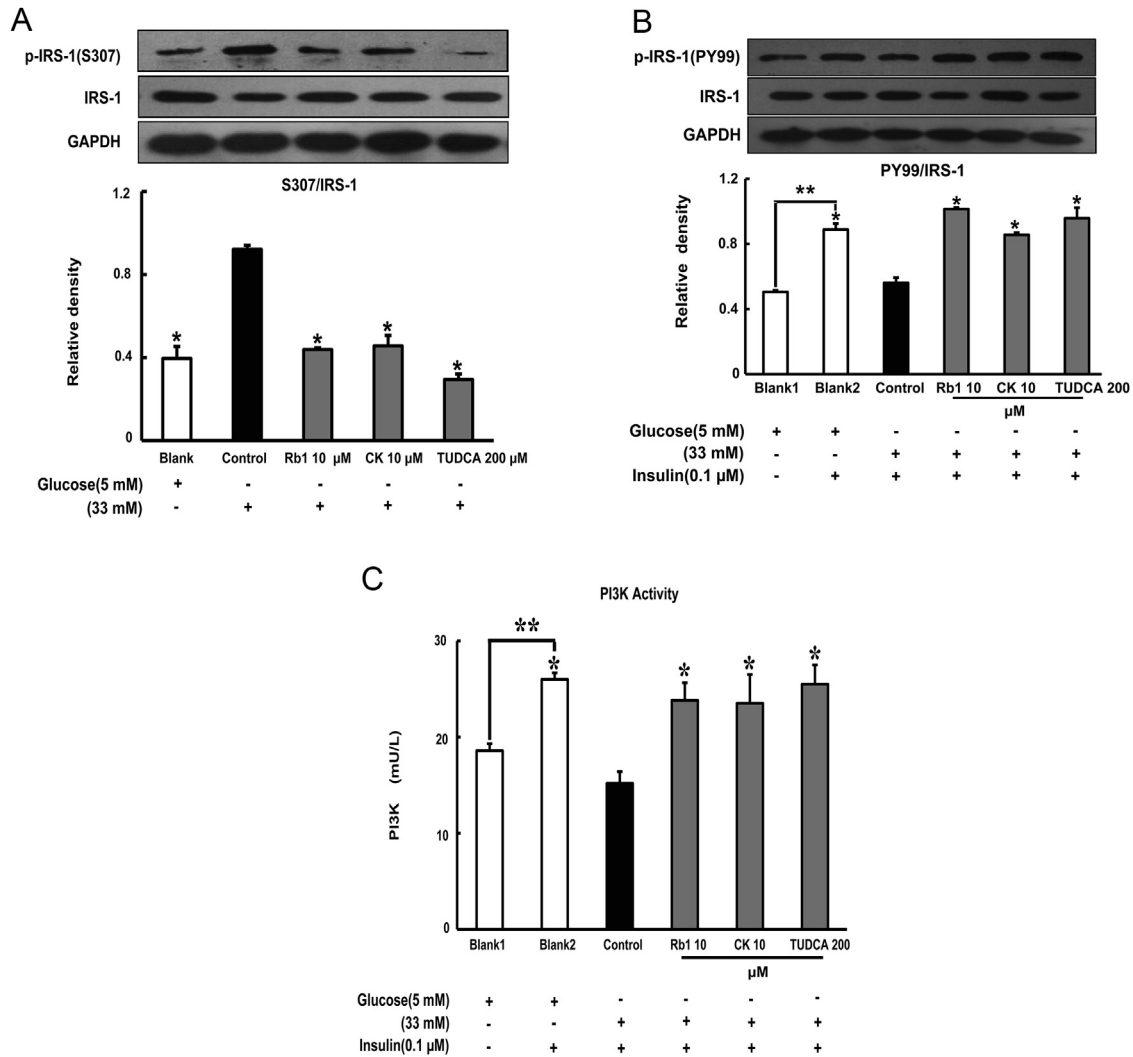
Fig. 7. Rb1 and CK modulate IRS-1 phosphorylation in the presence of high glucose concentrations. Epididymal adipose tissue was separated after the mice were scarified. The tissue was pretreated with Rb1, CK, or TUDCA at given concentrations, followed by stimulation with high glucose (33mM) for 24 h with or without insulin treatment for an additional 30 min. (A,B) Serine phosphorylation of IRS-1 (S307) and tyrosine phosphorylation IRS-1 (PY99), respectively, were determined by western blot. (C) The level of PI3K in the supernatant of lysed tissue was assayed with an ELISA kit. All results were derived from three independent experiments for the western blot or expressed as the mean $\pm$ SD ($n = 4$) for ELISA. $^{*}p < 0.05$ versus high glucose-only treatment; $^{**}p < 0.05$ versus the indicated treatment. CK, ginsenoside compound K; ELISA, enzyme-linked immunosorbent assay; SD, standard deviation; TUDCA, tauroursodeoxycholic acid.

combination of Rb1 and CK suppressed ROS production, reduced IL-1β secretion, and preserved Akt activation in response to insulin (Fig. 9A—C). These results showed that the efficiency of the Rb1 and CK combination was equal to the individual components in the protection of insulin signaling under ER-stress conditions.

4. Discussion

Inflammation plays an important role in the development of obesity and insulin resistance [21]. Although ER stress is involved in metabolic disorders and insulin resistance, the molecular pathway linking ER stress to insulin resistance is not well known. Here, we demonstrated that high glucose concentrations induced ROS-associated ER stress in adipose tissue, leading to NLRP3 inflammasome activation. Rb1 and CK suppressed ER stress-induced NLRP3 inflammasome activation and ameliorated insulin resistance by inhibiting inflammation.

The ER plays a vital role in maintaining cellular and metabolic homeostasis, which is very sensitive to metabolic factors, such as glucose and lipid load [22,23]. Overloaded glucose increases ROS

production through the NADPH oxidase pathway [24], and excessive ROS can evoke ER stress. However, enhanced unfolded protein response also leads to increased ROS production, exacerbating ER stress. Rb1 and CK inhibited glucose-induced ROS production, and then effectively suppressed ER stress, indicated by dephosphorylation of IRE1α and PERK. Rb1 and CK are capable of inhibiting oxidative stress [20,25], therefore, our results provided further evidence that their antioxidative activity contributed to the prevention of ER stress.

ROS-associated ER stress is responsible for TXNIP induction [9]. TXNIP was originally characterized as a thioredoxin (TRX)-binding protein that regulates the antioxidant function of TRX [11], and its induction was implicated in obesity and inflammation [26]. In response to ROS production, TXNIP is released from TRX and binds to NLRP3 to induce NLRP3 inflammasome activation [27]. Additionally, ER stress was shown to cause TXNIP induction through the PERK and IRE1α pathways [9]. In the present study, high glucose concentrations induced ROS-associated ER stress with TXNIP induction, and ER-stress inhibitor TUDCA inhibited TXNIP expression, indicating a role of ER stress in TXNIP induction. Consistent with
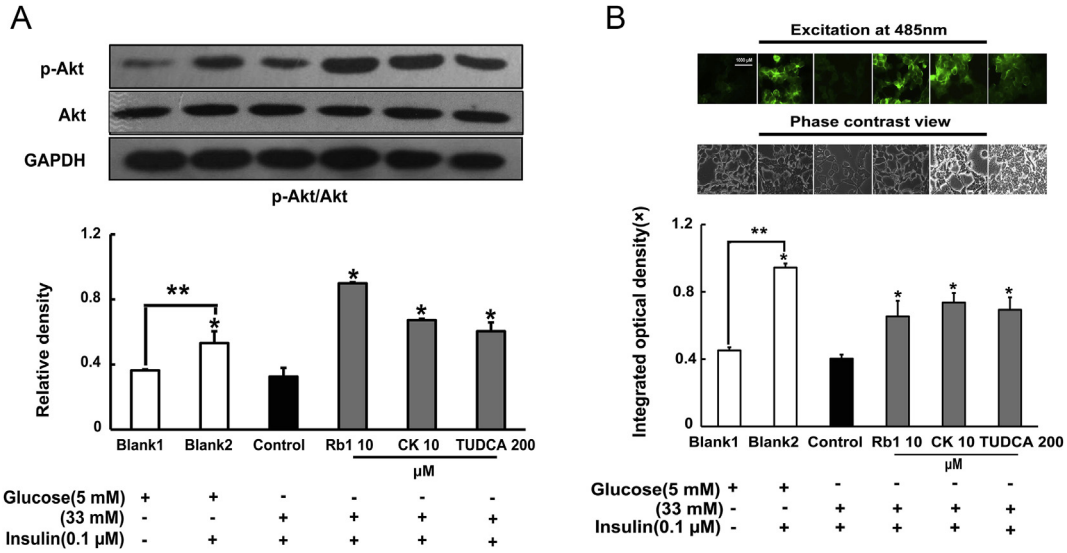
Fig. 8. Rb1 and CK enhance Akt phosphorylation and promote insulin-mediated glucose uptake in 3T3-L1 adipocytes. (A) Epididymal adipose tissue was separated and treated with Rb1, CK, or TUDCA, and cultured with high glucose concentrations with or without insulin treatment. Akt phosphorylation was detected by western blot. (B) After treatment with Rb1 and CK, 3T3-L1 adipocytes were incubated with 2-NDBG (0.5mM) and insulin (0.1μM), and fluorescence in cells was viewed by fluorescence microscope. Bar, 1000 μm. The results were expressed as the mean ± SD of three independent experiments. $*p < 0.05$ versus high glucose-only treatment; $** p < 0.05$ versus the indicated treatment. CK, ginsenoside compound K; SD, standard deviation; TUDCA, tauroursodeoxycholic acid.
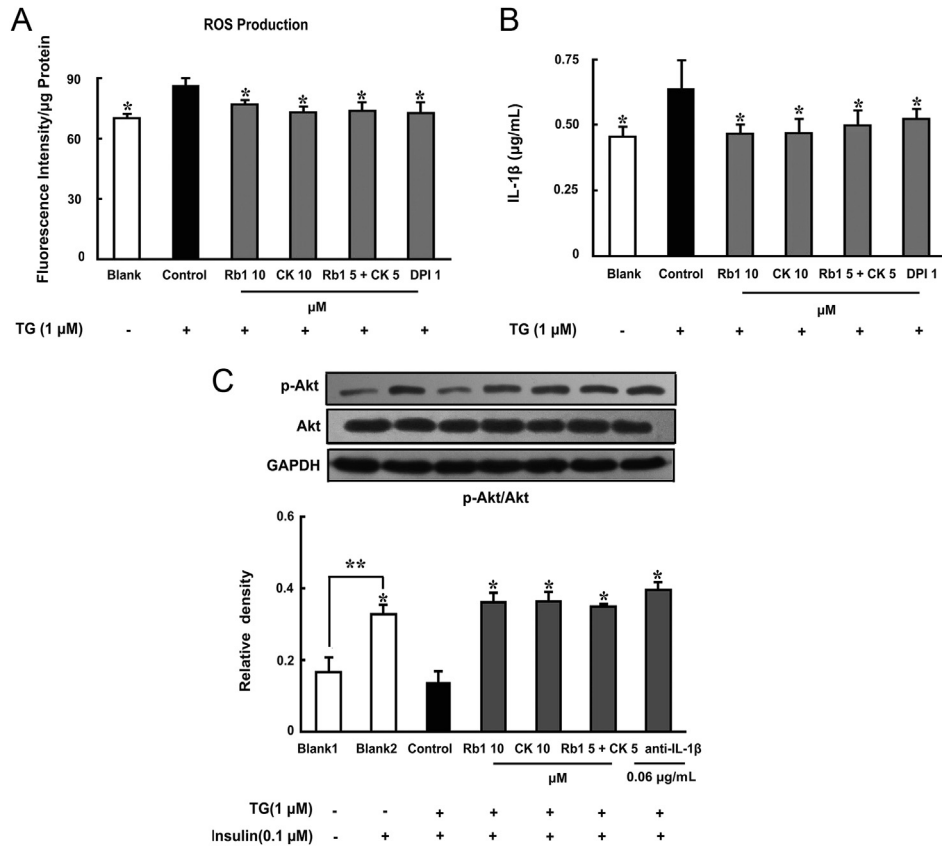
Fig. 9. The combination of Rb1 and CK improved insulin signaling. Epididymal adipose tissue was separated from mice, cultured with Rb1 (10μM), CK (10μM), Rb1 (5μM)+CK (5μM), DPI (1μM), or anti-IL-1β antibody (0.06 μg/mL), and then stimulated with TG (1μM) with or without insulin treatment. (A) ROS production in the tissue was determined by ROS-specific fluorescent-probe dye DCFH-DA by a microplate reader. (B) IL-1β in the supernatant was measured with an ELISA kit. (C) Akt phosphorylation was detected by western blot. Data were expressed as the mean ± SD from three independent experiments or as the mean ± SD ($n = 4$) for ELISA. $*p < 0.05$ versus TG-only treatment; $** p < 0.05$ versus the indicated treatment. CK, ginsenoside compound K; DCFH-DA, dichloro-dihydro-fluorescein diacetate; DPI, diphenyleneiodonium chloride; ELISA, enzyme-linked immunosorbent assay; ROS, reactive oxygen species; SD, standard deviation; TUDCA, tauroursodeoxycholic acid.

the functional connection, Rb1 and CK inhibited TXNIP induction, and thereby suppressed NLRP3 inflammasome activation, as indicated by attenuated NLRP3 expression and cleaved caspase-1 levels. NLRP3 inflammasome activation promotes IL-1β maturation following cleavage by caspase-1. By suppressing NLRP3 inflammasome activation, we observed reduced IL-1β secretion in adipose tissue subjected to Rb1 and CK treatment. To confirm the involvement of ER stress and oxidative stress in the initiation of inflammation, we observed that IL-1β secretion was upregulated in response to TG stimulation. This alteration was prevented by pretreatment with DPI, an inhibitor of NADPH oxidase. IL-6 is a major downstream product of IL-1β. Rb1 and CK prevented IL-1β maturation and secretion, thereby inhibiting IL-6 production. These results demonstrated the anti-inflammatory activity of Rb1 and CK in adipose tissue under ER-stress conditions.

Inflammation is a critical factor leading to insulin resistance, and Rb1 and CK inhibited inflammation by blocking inflammasome activation. We then questioned whether this action contributed to preventing insulin resistance in adipose tissue. Pro-inflammatory cytokines, including IL-1β, IL-6, and TNF-α, can impair IRS-1 function by increasing its phosphorylation, thus preventing insulin-mediated IRS-1 tyrosine phosphorylation [28]. In our study, Rb1 and CK inhibited inflammation by suppressing NLRP3 inflammasome activation. As expected, we observed that both agents effectively reduced IRS-1 serine phosphorylation and successfully restored insulin-mediated tyrosine phosphorylation, demonstrating their action in the protection of IRS-1 function against inflammatory insult. Furthermore, Rb1 and CK increased PI3K activity, preserved Akt activation, and therefore improved glucose uptake, demonstrating their beneficial effects on the improvement of insulin action in adipocytes. TUDCA, an ER-stress inhibitor, also improved the IRS-1/PI3K/Akt insulin signaling pathway and increased glucose uptake, indicating that suppression of ER stress contributed to the amelioration of insulin resistance by inhibition of inflammation. Anti-IL-1β antibody pretreatment also protected the insulin-induced phosphorylation of Akt against TG insult, further indicating the crucial role of ER stress-associated NLRP3 inflammasome activation in the development of insulin resistance.

Because CK is a product derived from Rb1 metabolism by intestinal bacteria after oral administration [14], and both compounds are present simultaneously in the blood, it was interesting to observe Rb1 and CK working together. The combination of Rb1 and CK exerted similar effects as those observed from Rb1 or CK individual treatment, suggesting that although Rb1 was converted to CK by intestinal metabolism, the protective effects of Rb1 were maintained. These results should be beneficial for increasing the understanding of ginsenoside activity in the management of metabolic disorders.

In conclusion, our work showed that ginsenoside Rb1 and its metabolite CK inhibited ER stress-associated TXNIP/NLRP3 inflammasome activation and ameliorated insulin resistance by inhibiting inflammation upon glucose stimulation. These findings offer a novel insight into the beneficial effects of ginsenosides on the regulation of glucose homeostasis, and promote their potential application toward the management of insulin resistance in obesity and diabetes.

Conflicts of interest

Acknowledgments

References

[1] Hager SR, Jochen AL, Kalkhoff RK. Insulin resistance in normal rats infused with glucose for 72 h. Am J Physiol 1991;260:E353—62.
[2] Rossetti L. Glucose toxicity: the implications of hyperglycemia in the pathophysiology of diabetes mellitus. Clin Invest Med 1995;18:255—60.
[3] Haber CA, Lam TK, Yu Z, Gupta N, Goh T, Bogdanovic E, Giacca A, Fantus IG. N-acetylcysteine and taurine prevent hyperglycemia-induced insulin resistance in vivo: possible role of oxidative stress. Am J Physiol Endocrinol Metab 2003;285:E744—53.
[4] Dedoussis GV, Kaliora AC, Panagiotakos DB. Genes, diet and type 2 diabetes mellitus: a review. Rev Diabet Stud 2007;4:13—24.
[5] Eizirik DL, Cardozo AK, Cnop M. The role for endoplasmic reticulum stress in diabetes mellitus. Endocr Rev 2008;29:42—61.
[6] Marciniak SJ, Ron D. Endoplasmic reticulum stress signaling in disease. Physiol Rev 2006;86:1133—49.
[7] Ringseis R, Eder K, Mooren FC, Krüger K. Metabolic signals and innate immune activation in obesity and exercise. Exerc Immunol Rev 2015;21:58—68.
[8] Schroder K, Tschopp J. The inflammasomes. Cell 2010;140:821—32.
[9] Oslowski CM, Hara T, O'Sullivan-Murphy B, Kanekura K, Lu S, Hara M, Ishigaki S, Zhu LJ, Hayashi E, Hui ST, et al. Thioredoxin-interacting protein mediates ER stress-induced β cell death through initiation of the inflammasome. Cell Metab 2012;16:265—73.
[10] Gual P, Le Marchand-Brustel Y, Tanti JF. Positive and negative regulation of insulin signaling through IRS-1 phosphorylation. Biochimie 2005;87:99—109.
[11] Zhou R, Tardivel A, Thorens B, Choi I, Tschopp J. Thioredoxin-interacting protein links oxidative stress to inflammasome activation. Nat Immunol 2010;11:136—40.
[12] Gao D, Madi M, Ding C, Fok M, Steele T, Ford C, Hunter L, Bing C. Interleukin-1β mediates macrophage-induced impairment of insulin signaling in human primary adipocytes. Am J Physiol Endocrinol Metab 2014;307: E289—304.
[13] Maedler K, Dharmadhikari G, Schumann DM, Størling J. Interleukin-1 beta targeted therapy for type 2 diabetes. Expert Opin Biol Ther 2009;9:1177—88.
[14] Akao T, Kida H, Kanaoka M, Hattori M, Kobashi K. Intestinal bacterial hydrolysis is required for the appearance of compound K in rat plasma after oral administration of ginsenoside Rb1 from Panax ginseng. J Pharm Pharmacol 1998;50:1155—60.
[15] Xiong Y, Shen L, Liu KJ, Tso P, Xiong Y, Wang G, Woods SC, Liu M. Antiobesity and antihyperglycemic effects of ginsenoside Rb1 in rats. Diabetes 2010;59: 2505—12.
[16] Shang W, Yang Y, Zhou L, Jiang B, Jin H, Chen M. Ginsenoside Rb1 stimulates glucose uptake through insulin-like signaling pathway in 3T3-L1 adipocytes. J Endocrinol 2008;198:561—9.
[17] Jiang S, Ren D, Li J, Yuan G, Li H, Xu G, Han X, Du P, An L. Effects of compound K on hyperglycemia and insulin resistance in rats with type 2 diabetes mellitus. Fitoterapia 2014;95:58—64.
[18] Park EK, Shin YW, Lee HU, Kim SS, Lee YC, Lee BY, Kim DH. Inhibitory effect of ginsenoside Rb1 and compound K on NO and prostaglandin E2 biosyntheses of RAW264.7 cells induced by lipopolysaccharide. Biol Pharm Bull 2005;28: 652—6.
[19] Joh EH, Lee IA, Jung IH, Kim DH. Ginsenoside Rb1 and its metabolite compound K inhibit IRAK-1 activation—the key step of inflammation. Biochem Pharmacol 2011;82:278—86.
[20] Kim S, Na JY, Song KB, Choi DS, Kim JH, Kwon YB, Kwon J. Protective effect of ginsenoside Rb1 on hydrogen peroxide-induced oxidative stress in rat articular chondrocytes. J Ginseng Res 2012;36:161—8.
[21] Roberts CK, Hevener AL, Barnard RJ. Metabolic syndrome and insulin resistance: underlying causes and modification by exercise training. Compr Physiol 2013;3:1—58.
[22] Cao SS, Kaufman RJ. Endoplasmic reticulum stress and oxidative stress in cell fate decision and human disease. Antioxid Redox Signal 2014;21:396—413.
[23] Zhang K, Kaufman RJ. From endoplasmic-reticulum stress to the inflammatory response. Nature 2008;454:455—62.
[24] Lambeth JD, Neish AS. Nox enzymes and new thinking on reactive oxygen: a double-edged sword revisited. Annu Rev Pathol 2014;9:119—45.
[25] Shao X, Li N, Zhan J, Sun H, An L, Du P. Protective effect of compound K on diabetic rats. Nat Prod Commun 2015;10:243—5.
[26] Mohamed IN, Hafez SS, Fairaq A, Ergul A, Imig JD, El-Remessy AB. Thioredoxin-interacting protein is required for endothelial NLRP3 inflammasome activation and cell death in a rat model of high-fat diet. Diabetologia 2014;57: 413—23.
[27] Mittal M, Siddiqui MR, Tran K, Reddy SP, Malik AB. Reactive oxygen species in inflammation and tissue injury. Antioxid Redox Signal 2014;20:1126—67.
[28] Aguirre V, Werner ED, Giraud J, Lee YH, Shoelson SE, White MF. Phosphorylation of Ser307 in insulin receptor substrate-1 blocks interactions with the insulin receptor and inhibits insulin action. J Biol Chem 2002;277: 1531—7.